Global observations of the carbon budget
3. Initial assessment of the impact of satellite orbit, scan geometry, and cloud on measuring CO$_2$ from space

P. J. Rayner, R. M. Law, and D. M. O'Brien
Atmospheric Research, Commonwealth Scientific and Industrial Research Organisation, Aspendale, Victoria, Australia

T. M. Butler
School of Earth Sciences, University of Melbourne, Parkville, Victoria, Australia

A. C. Dilley
Atmospheric Research, Commonwealth Scientific and Industrial Research Organisation, Aspendale, Victoria, Australia

[1]   In this third of three companion papers we assess the utility of column-integrated measurements of CO$_2$ in constraining surface source estimates. The measurements have error characteristics defined by *O'Brien and Rayner* [2002]. There we described a retrieval algorithm which appeared capable of unbiased retrievals. An assessment of the sensitivity to dominant sources of error in these measurements suggested a precision about 0.5% of the background mixing ratio. We include this information along with the probability of clear sky and the sampling pattern imposed by a particular orbit and scan geometry. We carry out a synthesis inversion to recover specified surface sources. The uncertainty of the inferred sources quantifies the strength of the constraint offered by such measurements. The difference between input and retrieved sources demonstrates biases in the whole procedure. We show that source uncertainties are low in the presence of a sunlit surface but rise dramatically at high latitudes in winter. Provided we use sufficient spatial resolution for the sources we estimate, the inversion can also produce relatively accurate estimates. The inversion procedure is sensitive to biases caused by poor sampling of the diurnal cycle. Errors that isotropically affect all measured mixing ratios do not cause biases in estimated sources.   *INDEX TERMS:* 0322 Atmospheric Composition and Structure: Constituent sources and sinks; 1640 Global Change: Remote sensing; 0394 Atmospheric Composition and Structure: Instruments and techniques; *KEYWORDS:* carbon dioxide, satellite, atmospheric inversion, near infrared, scan geometry

Citation: Rayner, P. J., R. M. Law, D. M. O'Brien, T. M. Butler, and A. C. Dilley, Global observations of the carbon budget, 3, Initial assessment of the impact of satellite orbit, scan geometry, and cloud on measuring CO$_2$ from space, *J. Geophys. Res.*, *107*(D21), 4557, doi:10.1029/2001JD000618, 2002.

1. Introduction

[2]   *O'Brien and Rayner* [2002] proposed a method for observing the column amount of CO$_2$ using a near infra-red radiometer measuring radiances in the 1.61 μm band for CO$_2$ and the 1.27 μm band for O$_2$. Their method relied on the correlated responses of scattered radiances in these bands to the presence of aerosol and thin cloud. This correlated response meant the impact of these contaminants on the estimate of column CO$_2$ amount could be reduced. The degradation in performance caused by uncertainty in cloud height could be largely removed if a second O$_2$ channel was also measured.

[3]   Their analysis included the impact of uncertainties in temperature, and the presence of aerosol and cloud. It did

not include uncertainties due to errors in spectroscopic properties or, critically, the impact of cloud obscuration on sampling. For a measurement in an atmosphere with total optical depth of aerosol and thin cloud less than approximately 0.3, however, they derived an error estimate which was unbiased (i.e. had zero mean). Thus, provided all the inputs to the retrieval procedure are specified correctly, the procedure will return a correct value of column CO$_2$ amount. Furthermore, a sensitivity analysis to the most likely sources of error in such retrievals suggested that reasonable uncertainties on input fields would yield a precision around 0.5% for the retrieved CO$_2$ column-integrated mixing ratio. We should keep in mind, though, that persistent errors in these input fields will yield persistent errors in the retrieval.

[4]   In this paper we will use the properties of these errors in a series of retrievals or inversions of the distribution of

surface fluxes. We also use a sampling distribution reflecting a potential instrument, orbit and scanning geometry along with the impact of cloud obscuration. In one sense the study is an extension of *Rayner and O'Brien* [2001] (hereinafter referred to as RO1). That study was deliberately generic, taking no particular account of the behavior of a satellite in sampling the atmosphere. That study also made no attempt to investigate the accuracy of the retrieved surface fluxes. Here we make some preliminary steps in that direction by recovering some known sources. Such so-called pseudodata experiments allow us to test some of the limitations of the approach but not others. Hence the paper should be considered part of an ongoing investigation; there are many causes of potential error we will not investigate here, principally errors in the simulation of atmospheric transport.

[5] In the next section we describe the satellite sampling of the atmosphere. We then describe how this data set is incorporated into the atmospheric transport model and describe the synthesis inversion procedure we use. We will show results for the uncertainty and bias of a control inversion. We also demonstrate the impact of two particular types of error which may occur in satellite data and discuss their implications for flux retrievals.

2. Simulations With Realistic Orbit and Scan Geometry

[6] We accept as a starting point the statistics (mean and variance) of the errors caused by atmospheric noise estimated by *O'Brien and Rayner* [2002]. To address the issues of orbit and scan geometry, we consider a hypothetical multichannel radiometer on a satellite in a sun-synchronous orbit with a northward equatorial crossing time of 10:30am local time. The satellite tracks the point of specular reflection or glitter on the earth's surface. It samples the radiance from this direction whenever the solar zenith angle is below some threshold, chosen here as 70°. The time between footprints is set at 5 s, based on a preliminary design of a tunable etalon spectrometer with high spectral resolution ($\approx$0.02 cm^{-1}) and high signal-to-noise ratio of 520.

[7] The probability of clear sky for land surfaces was determined through analysis of NOAA/NASA Pathfinder AVHRR Land (PAL) data [*James and Kalluri*, 1994]. Cloud flags produced by the CLAVR algorithm [*Stowe et al.*, 1999] were extracted for each pixel at 8 km × 8 km spatial resolution from a ten year archive of daily PAL data. The probability that the sky would be clear on any day in a selected month, say January, was obtained by counting the number of cloud free occurrences of the pixel over the ten year period and then dividing by the total number of January days. Over the oceans, monthly averages of cloud amount (*CA*) were taken from three years of International Satellite Cloud Climatology Project (ISCCP) data [*Rossow and Schiffer*, 1991] at 2.5° × 2.5° spatial resolution. Since *CA* is defined by ISCCP to be the ratio of the number of cloudy pixels to the total number of pixels within the grid cell, we have taken (1 − *CA*) to represent the probability that a pixel within the grid cell will be clear. In this calculation only 26% of available pixels were found to be cloud free.

[8] The simulations were carried out for one year, in which time approximately 746,000 clear pixels were obtained, of which 190,000 occurred over land and 556,000 over the oceans.

2.1. Simulating Orbits in a Transport Model

[9] Before we can use the satellite simulations in an atmospheric inversion we need to mimic them in the domain of a chemical transport model (CTM). We need to determine two things: first, the locations and times for sampling model mixing ratios and, second, the uncertainties we should include on each of these CTM samples.

[10] The orbit construction is carried out at much higher temporal and spatial resolution than the CTMs used for atmospheric inversion studies. The model we use has a time step of one hour and a spatial resolution of 5.6° longitude × 2.8° latitude. We consider a CTM grid cell to be observed at a given time step if any satellite observed pixel falls within it. We use the model mixing ratio in that grid cell as the sample value and assign an uncertainty according to the error model from *O'Brien and Rayner* [2002]. For a given source field this sampling strategy will produce a vector of mixing ratios sampled along the satellite track. With the orbital period we use (approx. 99 min), this vector may contain many samples each model time step. The field-of-view of the satellite is much smaller than the CTM grid cells and the integration time is short compared to the transit time of the satellite over a model grid cell. Thus depending on viewing conditions, a given model grid cell may be sampled several times during one overpass. We ignore this occurrence when constructing either the pseudodata or its uncertainty. The effect is significant; the approx. 746,000 satellite samples condense to approx. 234,000 model samples.

[11] Figure 1 shows the zonal mean of the number of model samples per grid cell for January and July respectively. The distribution is governed both by the occurrence of cloud and the restrictions imposed by solar zenith angle. As expected the high latitudes of the winter hemisphere are almost unobserved. The unobserved region in the northern hemisphere may include regions with significant industrial sources while important natural sources may occur in the high latitudes of either hemisphere. Limitation of sampling in winter will be common to any measurement technique using reflected sunlight.

[12] The simplicity of the sampling strategy we use is most important for the specification of the uncertainties used on the pseudodata within the inversion. The simplification ignores two compensating issues. First we make no attempt to consider the representativeness of the very small footprint of our satellite pixel for the CTM grid cell. This is obviously an optimistic assumption. To compensate we also do not reduce the error on the pseudodata used in the inversion according to the number of satellite "hits" in the grid cell. This is equivalent to assuming complete error correlation among the satellite observations in a grid cell and time step, so that extra observations add no more information. The relationship among these two effects is highly complex. It depends on the heterogeneity of sources in a grid cell, rates of horizontal diffusion of column-integrated tracer and the detail of the distribution of hits itself. It will require studies with high-resolution atmospheric models or, preferably, airborne instruments to determine the appropriate error model.
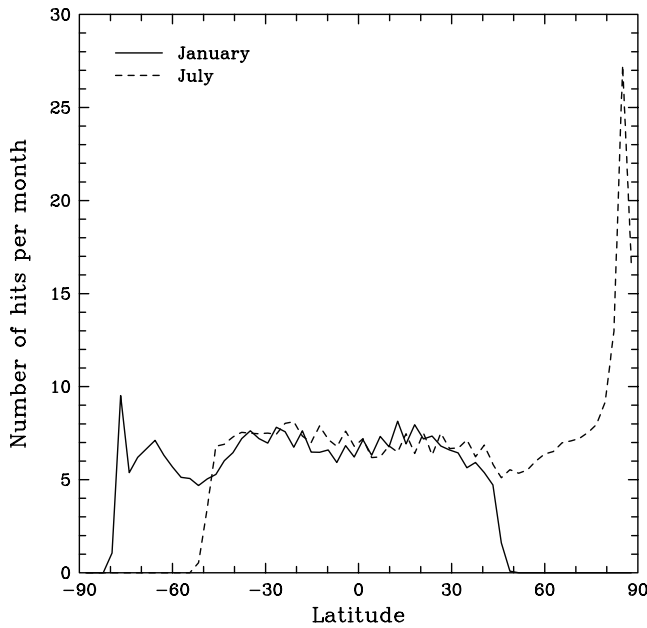
Figure 1. Zonal mean of the number of model samples per month per grid cell for the months of January (solid) and July (dashed).

[13] We also asume that errors on pseudodata are independent. This assumes that errors in the data required for the CO$_2$ retrieval are uncorrelated on scales larger than a CTM grid cell. This is perhaps true for some of the meteorological fields such as surface pressure. It is obviously not true for quantities such as spectroscopic properties. We will deal with this special case later.

2.2. Synthesis Inversion

[14] To test the potential utility of satellite data with these error characteristics, we performed several synthesis inversion calculations in which we attempted to recover the distribution of known sources. The generalities of the synthesis inversion technique are described by *Enting et al.* [1995] and *Rayner et al.* [1999]. Briefly the surface of the planet is divided into a number of regions. For each region, a unit source (often with a structure within the region) is input into a chemical transport model and the resulting mixing ratios sampled at chosen places and times. We refer to sources input to the transport model as the set of basis functions for the inversion and the mixing ratio samples generated for each one as the corresponding response functions. The magnitudes of the sources are then adjusted to match the data at the sampling locations. The linearity of mixing ratios with respect to sources (for inert tracers) allows us to use linear least squares fitting to produce an optimal match to the data.

[15] The fit returns not only an optimal estimate for sources but its uncertainty in the form of a covariance matrix. It is a general property of such linear fits that the covariance does not depend on the data itself. This property was used in RO1 to investigate the precision of source-sink estimates as a function of measurement precision. Here we perform a similar study with a number of important differences.

[16] First, the transport model is different. We use the CRC-MATCH CTM as used by *Law and Rayner* [1999] and

described by *Rasch et al.* [1997]. Second, the choice of regions is different. We use a subdivision of the 22 regions of *Gurney et al.* [2002]. We divide each region from that study into approximately 5 smaller regions. It was demonstrated by *Kaminski et al.* [2001] and *Law et al.* [2002] that the use of large source regions could seriously compromise the accuracy of inferred sources from an inversion. Since we ultimately wish to test the importance of other sources of error in such inferences we needed to reduce this bias to a reasonable level. We also wished to test the potential ability of satellite data to constrain sources on smaller scales than the near-continental regions in RO1.

[17] For our known or target source we use the same terrestrial biospheric source as *Gurney et al.* [2002] used. The fluxes represent the diurnally averaged terrestrial biospheric source as computed by the CASA model of *Potter et al.* [1993] and *Field et al.* [1995]. The lack of a diurnal cycle in the target field is an important restriction. We consider a simple sensitivity test here but a detailed analysis of the importance of diurnal bias is left to a future study. The target field also contains significant spatial variations within each basis function region, even though this study uses unusually high resolution for the source retrieval. It is a priori unclear whether the chosen source resolution is sufficient to overcome the biases associated with such unresolved variability. The temporal structure of the basis functions is also different from the target field. The basis functions are constant within each month while the target field is linearly interpolated from midmonthly values.

[18] We also make a different choice of prior uncertainty to RO1. That study aimed to compare the potential utility of satellite data with previous surface-based methods. These methods often rely heavily on prior information in regions with little data. Here, we are interested in the utility of the satellite data only, so we simplify the problem by choosing a prior uncertainty so large that the inversion is essentially unconstrained. To account for the very different sizes of regions we also choose a prior uncertainty proportional to region size. This has the effect of recasting the problem into a solution for the flux density from each region. For each month we choose a value of 0 ± 2000 gCm^{-2}yr^{-1}. The vastly different sizes of our basis function regions translates this into a range of 0.07 GtCyr^{-1} to 40.4 GtCyr^{-1}. Finally we need to specify the errors on the pseudodata used in the inversion. Following the discussion of sampling strategy and *O'Brien and Rayner* [2002], we choose a form of normally distributed uncorrelated errors with zero mean and a standard deviation of 1.8 ppm.

3. Results

[19] We first compare the uncertainties from this calculation with those from RO1. We summarize the uncertainty for each region using the root-mean-square uncertainty (RMSU) on the monthly mean sources. The RMSU for a given region j is defined as

$$\mathrm{RMSU}_j = \sqrt{\frac{\Sigma_1^{12}\sigma_{j,i}^2}{12}} \qquad (1)$$

where $\sigma_{j,i}$ is the uncertainty returned by the inversion for region j and month i. Note that this is a different and more
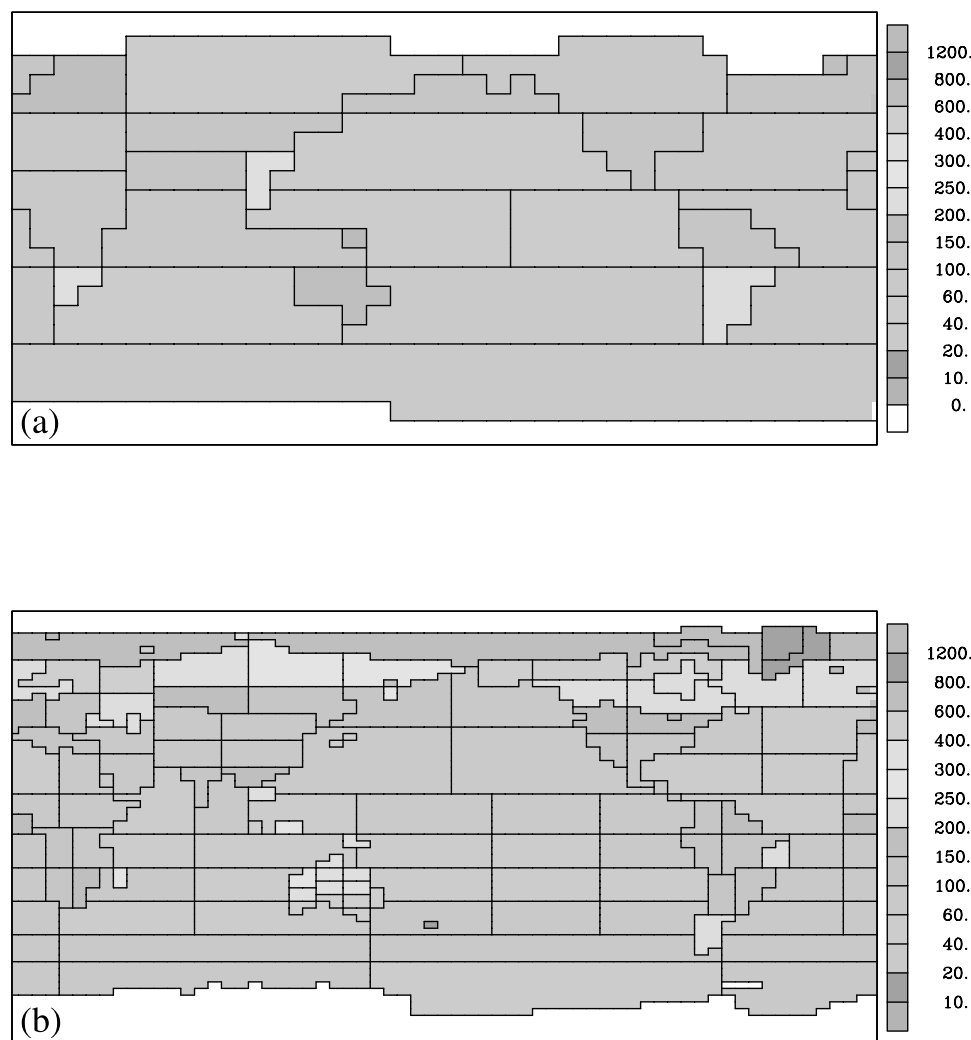
Figure 2. Root-mean square uncertainty ($gCm^{-2}yr^{-1}$) for the control calculation of (a) *Rayner and O'Brien* [2001] and (b) our control. See color version of this figure at back of this issue.

demanding measure than the quantity shown in Figures 1 and 2 of RO1. They showed the uncertainty on the annual mean flux. This annual uncertainty is reduced partly due to the process of averaging nearly independent monthly estimates. We must also take account of the different region sizes used in RO1 and this study. We do this by displaying the uncertainty as a flux density rather than the total emission for each region.

[20] We can further summarize the uncertainty in the area weighted RMSU. Table 1 lists this measure among others for these calculations. We see a 30% reduction in the integrated RMSU between the cases. Direct comparison is difficult but an approximate scaling argument would suggest RMSU scaling with the root of the number of regions, inversely as the root of the number of measurements and directly with the measurement precision. This suggests an approximate 25% improvement, close to the model result. This result is at first glance surprising. Our calculation uses data at relatively high time frequencies and hence has the capacity to use the synoptic variations in atmospheric flow to improve the localization of sources. This effect was previously noted by *Law et al.* [2002] who saw significant

improvement with the use of high time frequency atmospheric composition measurements made at the surface. We do see the same effect here but it is largely offset by contributions made to the integrated uncertainty by the unobserved high latitudes of the winter hemisphere. In fact if we rank the 1392 individual monthly estimates by their contribution to the integrated squared RMSU, half the total is provided by 72 estimates all of which are for regions poleward of ±50° latitude.

[21] Figure 2 shows the spatial structure of the RMSU for our control case and the 1 ppm data uncertainty case from RO1. The annual mean uncertainty for the RO1 case was shown as Figure 2 in that paper. Both plots show consid-

Table 1. Integrated Measures of Inversion Quality for the Cases Described in the Text

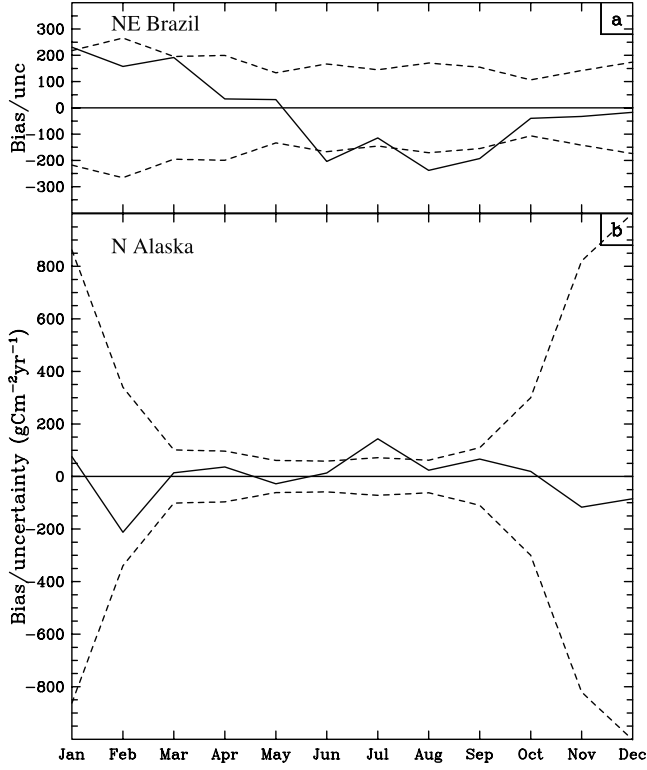| Name	Integrated RMSU, $GtCyr^{-1}$	Integrated RMSB, $GtCyr^{-1}$	Land-Ocean Bias, $GtCyr^{-1}$
RO1	7.1	n/a	n/a
Control	5.1	2.2	0.37
Diurnal	5.1	2.7	1.83
Spectroscopic	5.1	2.2	0.36

Figure 3. Bias (solid) and uncertainty (dashed) in gCm^{-2}yr^{-1} for regions in (a) Northeastern Brazil and (b) Northern Alaska. The uncertainty is shown as a band around the true solution (zero bias).

erable spatial structure. For RO1 this is caused mainly by different region sizes. There are two reasons for this: First, the prior uncertainty was specified as an emission uncertainty not an uncertainty in flux density so small regions have higher uncertainties when expressed as flux densities. Second, a small region will have fewer measurements situated within it and these measurements are the strongest constraint on the flux from a region. The first of these arguments does not hold for the new case. We chose a constant flux density uncertainty for the prior constraint. The second reason, region size, combines with the above-

mentioned poor constraint on high latitude regions in winter to explain the spatial structure in the new calculation.

[22] We can demonstrate the impact of the unobservable winter fluxes by considering the seasonal cycle of uncertainties for two regions, one in the high latitudes and one in the tropics. Figure 3 shows this along with the seasonal cycles in the bias (discussed shortly) for both regions. The uncertainty (dashed line) is shown as a band around zero (bias) so that it is easy to see when the bias moves outside the uncertainty range. We see a dramatic change in uncertainty in Northern Alaska with a factor of 10 difference between summer and winter. Seasonality in uncertainty for the tropical region is much smaller and is presumably driven by the seasonality in cloud cover.

[23] As well as measures of uncertainty, the pseudodata experiments allow us to comment on the biases in the inversion procedure caused either by the procedure itself or various corruptions of the data. Figure 4 shows the root mean square bias (RMSB) as a flux density. The RMSB is defined as

$$RMSB_j = \sqrt{\frac{\Sigma_1^{12}\left(F_{j,i}^m - F_{j,i}^t\right)^2}{12}} \qquad (2)$$

where $F_{j,i}^m$ and $F_{j,i}^t$ are respectively the modeled (inferred) and true fluxes for region j and month i.

[24] The RMSB is less than the RMSU for most regions providing some confidence in our inversion procedure. As with the RMSU we see some clear spatial structure in the RMSB. Most regions with very high uncertainties also show substantial biases. This suggests that various of the problems associated with the inversion procedure are more strongly manifest when the region is poorly constrained. However substantial biases are also seen for some of the larger (and hence better constrained) regions.

[25] We can summarize the bias analogously to the uncertainty using the area-integrated mean square bias. This is listed in Table 1. As expected from Figures 2 and 4 the integrated RMSB is less than the integrated RMSU. We infer from this that the biases inherent in the inversion procedure, mainly those due to the use of uniform sources over large regions, are tolerably small. We cannot infer
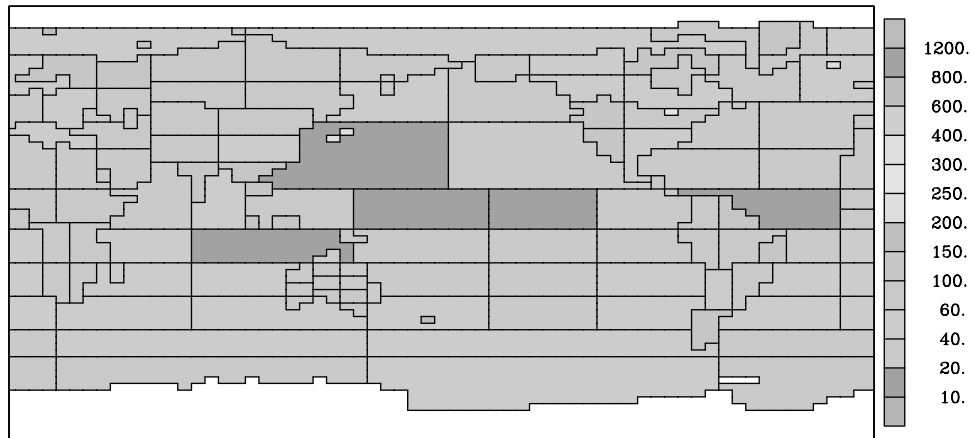

Figure 4. RMSB (gCm^{-2}yr^{-1}) for our control setup. See color version of this figure at back of this issue.

anything too general from this result since the spatial resolution required to recover particular sources will differ depending on the level of small-scale structure in the sources. The result does mean, however, that our inversion setup is sufficiently reliable to test the importance of corruptions in the data.

[26] Figure 3 shows the seasonal cycle in the bias for two chosen regions. We see a clear seasonal cycle in both regions. The errors are of quite different character however; in northern Alaska the inversion underestimates the seasonal cycle while it is overestimated in Brazil. Comparing the bias to the uncertainty points out months in which the inversion is most problematic. For example, although there is a large bias over Northern Alaska in February, this is associated with such a large uncertainty that we would place little weight on the inversion results. In contrast, the bias in July occurs despite the small uncertainty in the estimated flux.

[27] We now consider the impact of two different potential problems with satellite measurements. We summarize the results in Figure 5 which shows the zonal mean of the RMSB for both sensitivity experiments compared to the control. The first experiment considers the potential for a difference between the satellite measurements and the diurnal average. Such differences arise from the relatively large diurnal cycle in photosynthesis of plants. The diurnal cycle is seen over land rather than ocean because the large carbon reservoir in the surface ocean smooths such variations. Since the satellite samples at a fixed time of day the measured mixing ratios are prone to a bias with respect to the diurnal mean. If we imagine we are recovering diurnally averaged sources directly from the satellite measurements we may also bias our source estimates. In our sensitivity experiment we increase all the pseudodata from land points by 0.1 ppm. This represents an order of magnitude estimate of the daily productivity of the global land surface.

[28] In the second sensitivity case we roughly simulate the impact of an overall error in recovering CO$_2$ mixing ratio. This might occur, for example, from an error in spectroscopic parameters which affects every measurement. We simulate this by increasing every pseudodatum by 1%. Both experiments show only slight increases in the zonal mean RMSB compared to the control. The major reason for this is that the biases in the control case are randomly distributed and so the perturbation improves about as many estimates as it damages. The visual impression is borne out by the global integrals in Table 1.

[29] However the result for the diurnal bias experiment looks much more serious when we consider biases in flux integrated over large regions. The final column in Table 1 shows the integrated flux from the land. The control case yields 0.37 GtCyr^{-1}, which is reasonable. The diurnal bias case, however, produces a bias of 1.8 GtCyr^{-1}. This occurs since the inversion must now place a source over land sufficient to maintain the small but persistent gradient between land and ocean. Mass balance requires a corresponding sink over the ocean. We stress that this is a sensitivity experiment but it does suggest that the diurnal bias must be accounted for in estimating fluxes from such measurements.

[30] Unlike the diurnal bias case there is also no real change in the bias of the integrated flux in the second experiment. The reason for this invariance is relatively simple. The inversion procedure involves the estimation
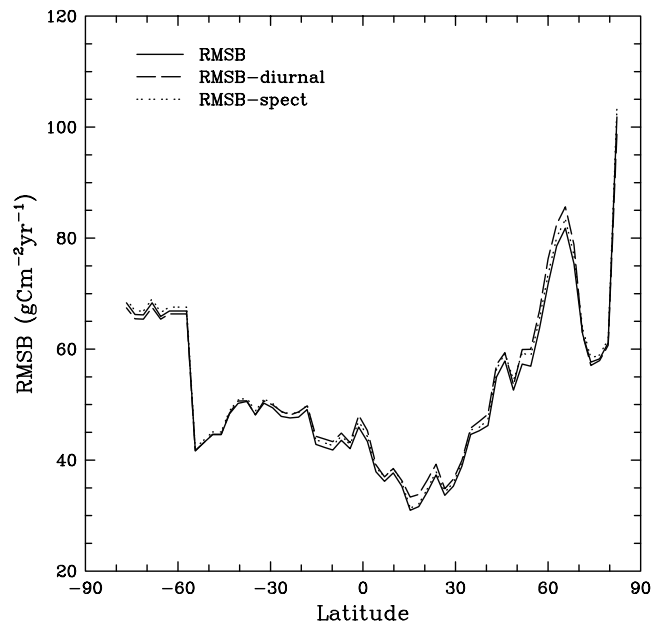

Figure 5. Zonal mean RMSB (gCm^{-2}yr^{-1}) for the control (solid) and the two sensitivity experiments (dashed, dotted).

of a global mean CO$_2$ mixing ratio. This is necessary to avoid sampling biases in the heterogeneous mixing ratio field from biasing our estimates. A useful side-effect is that the inversion is relatively insensitive to simple scaling of the mixing ratio field. The change is absorbed into a new estimate of this offset. This is clearly evident in this case with the offset increasing by almost exactly the 1% change in the data.

4. Discussion

[31] The above results form an early step in testing the encouraging but completely theoretical result of RO1. The results are mixed. From the viewpoint of the uncertainty of retrieved fluxes (the only metric considered in RO1) the results suggest good estimates are available over sunlit surfaces. The high uncertainties demonstrated for high latitudes in winter point out some important limitations of a passive instrument. Clearly a combined strategy involving surface and satellite measurements is required to obtain reasonable estimates throughout the year. Where measurements are available, the results suggest that useful information can be retrieved at higher spatial resolution than the large regions in RO1. In fact this higher spatial resolution is necessary to avoid serious biases in the inversion procedure itself. However even this result needs some important qualification. The most obvious is the simplicity of the error model used for the data. Similar scaling arguments as those in the previous section would suggest that a reduction in the effective number of measurements by a factor of two would produce similar integrated uncertainties in our control as for RO1. Such a reduction seems likely given correlation among errors. This does not mean the calculation is degraded to the level of RO1 since the extra detail in the flux estimates remains.

[32] Regarding potential biases the results look less satisfactory. The calculation we performed is intended as a

sensitivity test only; the magnitude of the problem in reality will depend on the amplitude of the diurnal cycle in mixing ratio. Also, several steps are available to ameliorate the problem. Most obvious is to include some simple model of the diurnal cycle to account for the bias. It is probably true that most of the diurnal variation is predictable and can hence, in principle, be treated as a deterministic forcing in the inversion, thus lessening the bias without greatly magnifying the uncertainty. An approach that does not rely on an external model is to treat the diurnal bias itself as part of the inversion so that we estimate it on some regional and temporal scale. This will absorb the potential bias in much the same way as the global offset absorbed the uncertainty in the absolute magnitude of the measurements. This solution risks dilution of the information content in spatial gradients of mixing ratio, since part of these gradients will be explained by an unknown diurnal bias. Finally, it is the sun-synchronous nature of the orbit which makes the diurnal bias in the data so consistent. Although a passive instrument can only sample during sunlight, it is possible that sampling across a broader range of the diurnal cycle may reduce the magnitude of the bias. This could be accomplished using a precessing orbit.

[33] We should also make two more general points on biases like the diurnal case. First, their importance depends on how one is treating the data. Figure 5 showed relatively small changes in the RMSB, suggesting that, for example, the amplitude of the seasonal cycle was not much affected by the problem. This amplitude is an important indicator of the activity of the terrestrial biosphere. It has already been used in diagnostic studies of the terrestrial biosphere [e.g., *Kaminski et al.*, 2002]. Also the diurnal bias problem is potentially common to all inversions using data from continental regions. Traditional flask sampling, for example, is also likely to produce uneven sampling of the diurnal cycle. The problem may be even more serious for surface measurements since the diurnal cycle of vertical transport will amplify the sampling bias.

[34] The general point that measurement issues cannot be separated from the detail of how the data will be used is also evident in the other data perturbation case. Here, even though errors in the absolute measurements are large, their structure makes them easy to remove. In fact, the procedure for estimating fluxes automatically accounts for this error. To generalize the point, such a measurement error is included in the statistical model that underlies the inversion. Other potential measurement problems can be incorporated similarly provided we can characterize their statistical behavior. We should keep in mind though that each error so treated will decrease the power of the measurements to estimate fluxes.

5. Conclusions

[35] The principal conclusion of this paper is that the limitations imposed by orbit, scan geometry and cloud cover do not appear to invalidate the result of RO1. In particular the direct use of the data continuously returned from the satellite (rather than its condensation into monthly means) allows us to estimate sources at higher spatial resolution than RO1 attempted. The impact of various

potential errors in such data is highly dependent on the way such data is incorporated into the process for estimating fluxes. As examples, a small bias over land, mimicking the diurnal bias of the measurements, seriously distorts large-scale integrated fluxes. However the potential for global errors in the concentration retrieval is included in the inversion formalism so does not impact the inversion. This suggests that meaningful use of such data will require close collaboration between those generating and using the data. Finally, the next stage in the evolution of this work should be to use a dynamical model of atmosphere and biosphere to predict the atmospheric composition and state. We can then calculate radiances from such a model and apply an inversion algorithm such as that proposed by *O'Brien and Rayner* [2002] to estimate CO$_2$ column amount. This should provide a more realistic picture of likely errors, especially their correlation in space and time.

References

Enting, I. G., C. M. Trudinger, and R. J. Francey, A synthesis inversion of the concentration and δ^{13}C of atmospheric CO$_2$, *Tellus, Ser. B*, *47*, 35–52, 1995.

Field, C. B., J. T. Randerson, and C. M. Malmström, Ecosystem net primary production: Combining ecology and remote sensing, *Remote Sens. Environ.*, *51*, 74–88, 1995.

Gurney, K. R., et al., Towards robust regional estimates of CO$_2$ sources and sinks using atmospheric transport models, *Nature*, *415*, 626–630, 2002.

James, M. E., and S. N. V. Kalluri, The Pathfinder AVHRR land data set: An improved coarse resolution data set for terrestrial monitoring, *Int. J. Remote Sens.*, *15*, 3347–3363, 1994.

Kaminski, T., P. J. Rayner, M. Heimann, and I. G. Enting, On aggregation errors in atmospheric transport inversions, *J. Geophys. Res.*, *106*, 4703–4715, 2001.

Kaminski, T., W. Knorr, P. Rayner, and M. Heimann, Assimilating atmospheric data into a terrestrial biosphere model: A case study of the seasonal cycle, *Global Biogeochem. Cycles*, *16*, doi:10.1029/2001GB001463, in press, 2002.

Law, R. M., and P. J. Rayner, Impacts of seasonal covariance on CO$_2$ inversions, *Global Biogeochem. Cycles*, *13*, 845–856, 1999.

Law R. M., P. J. Rayner, L. P. Steele, and I. G. Enting, Using high temporal frequency data for CO$_2$ inversions, *Global Biogeochem. Cycles*, *16*(4), 1053, doi:10.1029/2001GB001593, 2002.

O'Brien D. M., and P. J. Rayner, Global observations of the carbon budget, 2, CO$_2$ concentrations from differential absorption of reflected sunlight in the 1.61 μm band of CO$_2$, *J. Geophys. Res.*, *107*(D18), 4354, doi:10.1029/2001JD000617, 2002.

Potter, C. S., J. T. Randerson, C. B. Field, P. A. Matson, P. M. Vitousek, H. A. Mooney, and S. A. Klooster, Terrestrial ecosystem production: A process model based on global satellite and surface data, *Global Biogeochem. Cycles*, *7*, 811–841, 1993.

Rasch, P. J., N. M. Mahowald, and B. E. Eaton, Representations of transport, convection and the hydrologic cycle in chemical transport models: Implications for the modeling of short lived and soluble species, *J. Geophys. Res.*, *102*, 28,127–28,138, 1997.

Rayner, P. J., and D. M. O'Brien, The utility of remotely sensed CO$_2$ concentration data in surface source inversions, *Geophys. Res. Lett.*, *28*, 175–178, 2001.

Rayner, P. J., I. G. Enting, R. J. Francey, and R. Langenfelds, Reconstructing the recent carbon cycle from atmospheric CO$_2$, δ^{13}C and O$_2$/N$_2$ observations, *Tellus, Ser. B*, *51*, 213–232, 1999.

Rossow, W. B., and R. A. Schiffer, ISCCP cloud data products, *Bull. Am. Meteorol. Soc.*, *72*, 2–20, 1991.

Stowe, L. L., P. A. Davis, and E. P. McClain, Scientific basis and initial evaluation of the CLAVR-1 global clear/cloud classification algorithm for the AVHRR, *J. Atmos. Oceanic Technol.*, *16*, 656–681, 1999.

————————————

T. M. Butler, School of Earth Sciences, University of Melbourne, Parkville, Victoria 3010, Australia. (tmb@earthsci.unimelb.edu.au)

A. C. Dilley, R. M. Law, D. M. O'Brien, and P. J. Rayner, CSIRO Atmospheric Research, Private Bag 1, Aspendale, Victoria 3195, Australia. (peter.rayner@csiro.au)
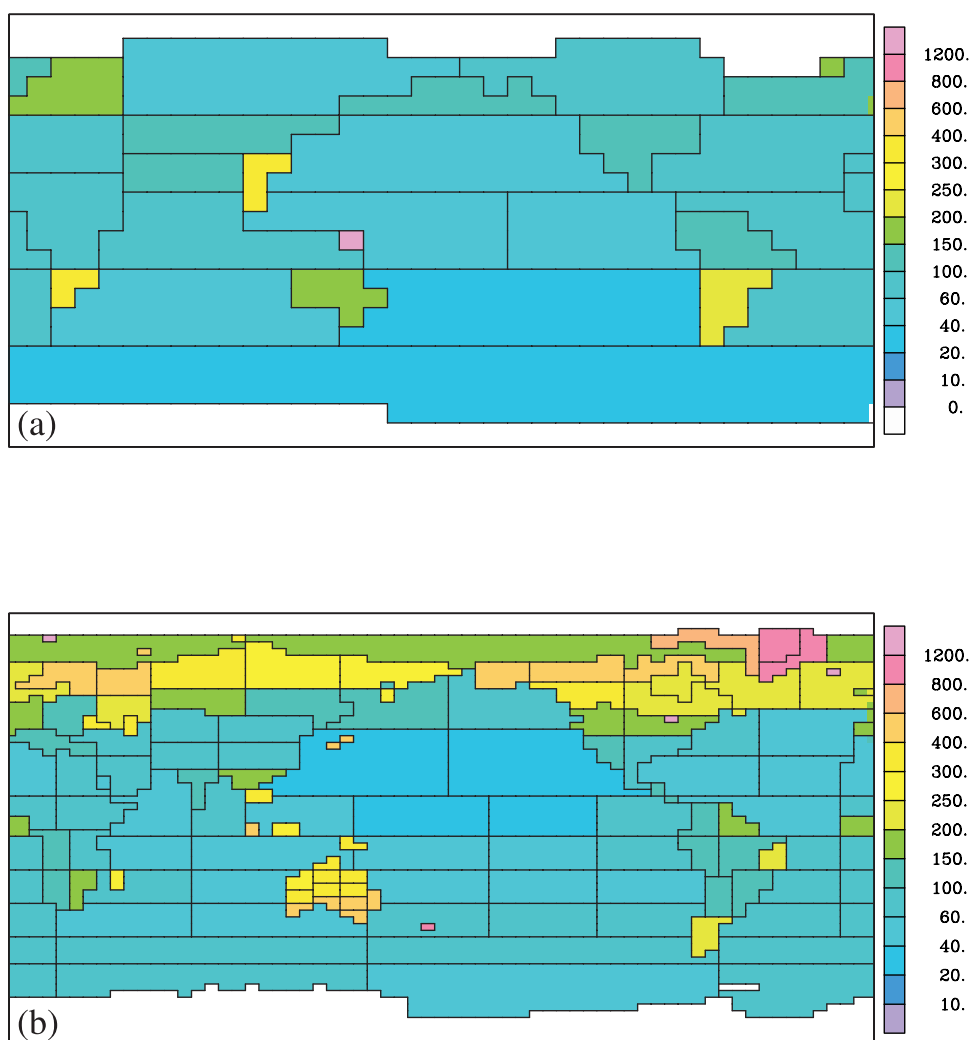
Figure 2. Root-mean square uncertainty (gCm^{-2}yr^{-1}) for the control calculation of (a) *Rayner and O'Brien* [2001] and (b) our control.
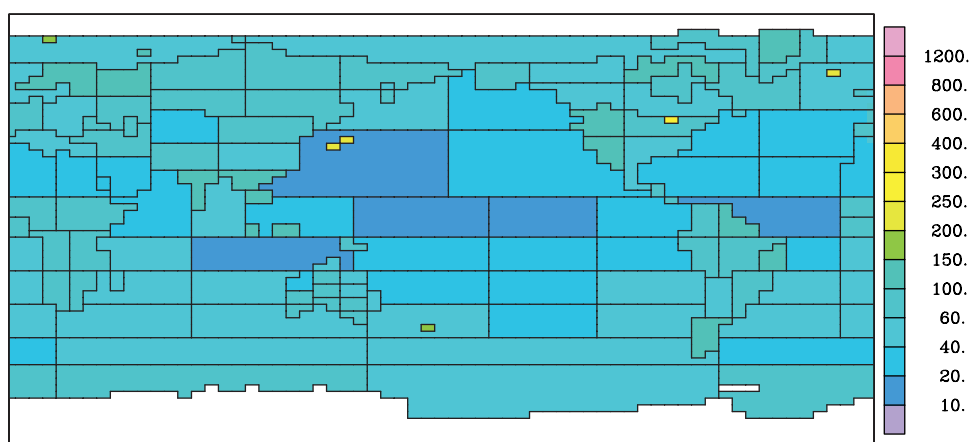

Figure 4. RMSB (gCm^{-2}yr^{-1}) for our control setup.